Taylor & Francis
Taylor & Francis Group

Journal of Enzyme Inhibition and Medicinal Chemistry

ISSN: 1475-6366 (Print) 1475-6374 (Online) Journal homepage: http://www.tandfonline.com/loi/ienz20

Cyclopropane-1,2-dicarboxylic acids as new tools for the biophysical investigation of O-acetylserine sulfhydrylases by fluorimetric methods and saturation transfer difference (STD) NMR

Giannamaria Annunziato, Marco Pieroni, Roberto Benoni, Barbara Campanini, Thelma A. Pertinhez, Chiara Pecchini, Agostino Bruno, Joana Magalhães, Stefano Bettati, Nina Franko, Andrea Mozzarelli & Gabriele Costantino

To cite this article: Giannamaria Annunziato, Marco Pieroni, Roberto Benoni, Barbara Campanini, Thelma A. Pertinhez, Chiara Pecchini, Agostino Bruno, Joana Magalhães, Stefano Bettati, Nina Franko, Andrea Mozzarelli & Gabriele Costantino (2016): Cyclopropane-1,2-dicarboxylic acids as new tools for the biophysical investigation of O-acetylserine sulfhydrylases by fluorimetric methods and saturation transfer difference (STD) NMR, Journal of Enzyme Inhibition and Medicinal Chemistry, DOI: 10.1080/14756366.2016.1218486

To link to this article: http://dx.doi.org/10.1080/14756366.2016.1218486

Published online: 31 Aug 2016.

Submit your article to this journal

Article views: 14

View related articles

View Crossmark data

Full Terms & Conditions of access and use can be found at
http://www.tandfonline.com/action/journalInformation?journalCode=ienz20

Download by: [York University Libraries] **Date:** 21 September 2016, At: 00:30

Journal of Enzyme Inhibition and Medicinal Chemistry

www.tandfonline.com/ienz
ISSN: 1475-6366 (print), 1475-6374 (electronic)

J Enzyme Inhib Med Chem, Early Online: 1–10
© 2016 Informa UK Limited, trading as Taylor & Francis Group. DOI: 10.1080/14756366.2016.1218486

Taylor & Francis
Taylor & Francis Group

ORIGINAL ARTICLE

Cyclopropane-1,2-dicarboxylic acids as new tools for the biophysical investigation of *O*-acetylserine sulfhydrylases by fluorimetric methods and saturation transfer difference (STD) NMR

Giannamaria Annunziato[1]*, Marco Pieroni[1]*, Roberto Benoni[4], Barbara Campanini[1], Thelma A. Pertinhez[2,3], Chiara Pecchini[1], Agostino Bruno[1], Joana Magalhães[1], Stefano Bettati[4,5], Nina Franko[1], Andrea Mozzarelli[1,5,6], and Gabriele Costantino[1]

[1]*Department of Pharmacy, and* [2]*Department of Biochemical, Biotechnological and Translational Sciences, University of Parma, Parma, Italy,* [3]*Transfusion Medicine Unit, ASMN-IRCCS, Reggio, Emilia, Italy,* [4]*Department of Neurosciences, University of Parma, Parma, Italy,* [5]*National Institute of Biostructures and Biosystems, Rome, Italy, and* [6]*Institute of Biophysics, CNR, Pisa, Italy*

Abstract

Cysteine is a building block for many biomolecules that are crucial for living organisms. *O*-Acetylserine sulfhydrylase (OASS), present in bacteria and plants but absent in mammals, catalyzes the last step of cysteine biosynthesis. This enzyme has been deeply investigated because, beside the biosynthesis of cysteine, it exerts a series of "moonlighting" activities in bacteria. We have previously reported a series of molecules capable of inhibiting Salmonella typhimurium (*S. typhymurium*) OASS isoforms at nanomolar concentrations, using a combination of computational and spectroscopic approaches. The cyclopropane-1,2-dicarboxylic acids presented herein provide further insights into the binding mode of small molecules to OASS enzymes. Saturation transfer difference NMR (STD-NMR) was used to characterize the molecule/enzyme interactions for both OASS-A and B. Most of the compounds induce a several fold increase in fluorescence emission of the pyridoxal 5′-phosphate (PLP) coenzyme upon binding to either OASS-A or OASS-B, making these compounds excellent tools for the development of competition-binding experiments.

Keywords

O-Acetylserine sulfhydrylase, cyclopropane-1,2-dicarboxylic acids, cysteine biosynthesis, drug resistance, saturation transfer difference-NMR

History

Received 28 June 2016
Revised 25 July 2016
Accepted 26 July 2016
Published online 25 August 2016

Introduction

Cysteine biosynthesis is carried out by bacteria and plants through the so-called reductive sulfate assimilation pathway (RSAP)[1,2]. The RSAP starts with the transport of sulfate inside the cell, followed by its reduction to bisulfide. Sulfur is then incorporated into cysteine via the reactions catalyzed by the last two enzymes of RSAP: serine acetyltransferase (SAT) and *O*-acetylserine sulfhydrylase (OASS). The former catalyzes the transfer of an acetyl group from acetyl-CoA to the hydroxyl of L-serine, leading to the formation of an activated form of serine, *O*-acetyl-L-serine (OAS) and CoA-SH. The latter enzyme catalyzes a two-step reaction: in the first half-reaction, an α-aminoacrylate is formed upon β-elimination of substituted L-serine; in the second half-reaction, the α-aminoacrylate is attacked by sulfide or other sulfur sources to give L-cysteine[3,4]. OASS is a pyridoxal 5′-phosphate (PLP)-dependent enzyme that in bacteria is present in two isoforms, conventionally referred to as OASS-A and OASS-B, coded by *cysK* and *cysM*, respectively. In enteric bacteria, OASS-A is highly expressed at basal levels, and so far, no conditions have been identified where OASS-B expression exceeds that of OASS-A[5], including anaerobic conditions that were previously reported to induce expression of the B isoform[6,7]. Cysteine biosynthesis is particularly important for a large number of microorganisms, especially during infection, when bacteria face the oxidative stress conditions induced by the host immune response. Indeed, it has been demonstrated that deletion of genes belonging to the cysteine biosynthetic pathway leads to a bacterial phenotype with reduced virulence, compromised fitness and a susceptibility to antibiotics several fold higher than the wild strains[8,9]. The recent disclosure of a number of additional moonlighting activities of OASS, specifically for OASS-A isoform, that is, toxin activation in some strains of *Escherichia coli* (*E. coli*)[10], gene expression in *Bacillus subtilis* (*B. subtilis*)[11], and the involvement of the enzyme in some pathologically relevant processes as the formation of biofilm and swarming motility, has further focused the interest of researchers toward these proteins[11–18]. These activities span from toxin activation in contact-dependent growth inhibition of uropathogenic *E. coli* strains[10], to gene expression in *B. subtilis*[11] and the involvement of the enzyme in some pathologically-relevant processes as the formation of biofilm and swarming motility[19]. Considering that mammals synthesize cysteine via a metabolic pathway that involves enzymes different from those present in RSAP, inhibitors of bacterial cysteine biosynthesis might be able to potentiate

*These authors contributed equally to this work.

Address for correspondence: Marco Pieroni, Department of Pharmacy, University of Parma, Parma, 43124, Italy. E-mail: marco.pieroni@unipr.it Barbara Campanini, Deparment of Pharmacy, University of Parma, Parma 43124, Italy. E-mail: barbara.campanini@unipr.it

antibiotic-based therapies[20]. Over the years, along with other groups[20,21], we have investigated structural and functional properties of OASS isozymes with the aim of further characterizing the biological features of these proteins and to explore the possibility of their inhibition by small molecules. The rational design of the first inhibitors was based on the structure of SAT, that physiologically inhibits OASS activity upon formation of the cysteine synthase bioenzyme complex[22,23]; in particular, it was considered that the carboxylic moiety of Ile267 of SAT is essential for the interaction between the two proteins[22–24]. Therefore, combining a structure-based with a ligand-based drug design approach, we planned and synthesized a series of cyclopropanecarboxylic acid derivatives that bind to both OASS isoforms at nanomolar concentrations[25–27]. In order to further refine the structure–activity relationships (SAR) around this class of derivatives, we herein report the design and synthesis of a series of cyclopropane-1,2-dicarboxylic acids variously functionalized. Although the binding properties of the previously reported analogs[24–26] could not be improved, the set of compounds herein presented provides interesting insight into the mode of binding of small molecules to OASS enzymes. In particular, saturation transfer difference NMR (STD-NMR) was used to further characterize the molecule/enzyme interactions for both OASS-A and B. Interestingly, most of the compounds induce a several fold increase in fluorescence emission of the pyridoxal 5′-phosphate (PLP) coenzyme upon binding to either OASS-A or OASS-B, likely due to changes in the polarity of the active-site microenvironment. This property, together with the modest binding affinity, makes these compounds excellent tools for the development of competition binding experiments. This is especially useful for the rapid and accurate determination of dissociation constants for other classes of ligands that either do not induce large changes of PLP fluorescence emission intensity, or bind with extremely high affinity, that is, behaving as tight binding inhibitors in the protein concentration range accessible to spectroscopic experiments.

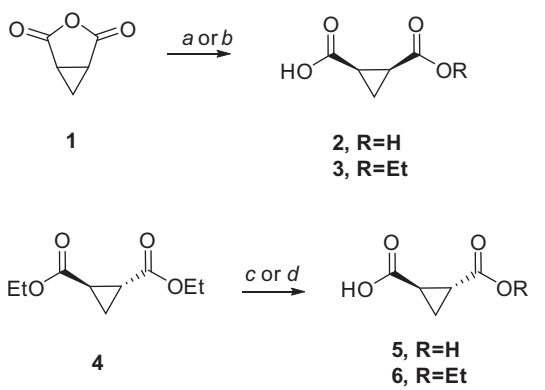

Scheme 1. [a]Reagents and conditions: (a) H_2O, reflux, 2 h, 98%; (b) EtOH, pyr, reflux, 12 h, 96%; (c) 1. 6N NaOH, reflux, 12 h, 2. aq. HCl, pH 2-3, 97%; (d) 14N NaOH (1 equiv.), EtOH, reflux, 15 min, 98%; [b]For complete structures (Table 1).

Methods

Synthetic chemistry

The synthesis of title *cis*-cyclopropane-1,2-carboxylic acid derivatives started from commercially available 3-oxabicyclo[3.1.0]hexane-2,4-dione, which was hydrolyzed with either water or ethanol to give, respectively, compounds **2** and **3** in good overall yields (Scheme 1). To obtain the *trans*-cyclopropane-1,2-carboxylic acid derivatives, diethyl (*1R,2R*)-cyclopropane-1,2-dicarboxylate was hydrolyzed in the presence of stoichiometric amount of potassium hydroxide, to give derivatives **5** and **6** in quantitative yields. For the synthesis of substituted cyclopropane-1,2-dicarboxylic acids (Scheme 2), key intermediates **13**–**18** were prepared according to a protocol described by McCoy[28,29], since the procedures already set by us proved to be not efficient[30,31]. Therefore, the suitable acrylates and α-halo esters were reacted in the presence of NaH, and the diethyl *cis*-cyclopropane-1,2-dicarboxylates were obtained. The subsequent hydrolysis in basic aqueous media afforded the title products **19**–**25** in good overall yields. Of note, during the cyclopropanation, the solvent plays a key role in the stereochemistry of the resulting molecules, with toluene being the best in conferring the desired *cis* configuration. Reacting benzyl cyanide and epichlorohydrin in the presence of sodium amide, at 90 °C in benzene, the corresponding cyclopropyl alcohol was obtained, that on turn underwent basic hydrolysis to give the title compound **28** in 44% overall yields (Scheme 3). Attempts to synthesize the ethyl ester of **28** according to other reported procedures[27,30] failed to give the desired compound.

NMR measurements for STD experiments

NMR spectra were acquired on a Varian (Agilent Technologies, Santa Clara, CA) Inova 600 NMR Spectrometer at 20 °C, on samples with a molar excess of 1:300. Ligand concentration was kept at 3 mM in the presence of 10 μM protein and were dissolved in phosphate buffer pH 8.0 (5 mM K_2PO_4, 3% DMSO-d_6).

Saturation transfer difference (STD) experiments were collected with 64 K data points in the direct dimension and 512 scans in a spectral window of 7000 Hz. The water signal was suppressed by the excitation sculpting method (dpfgse_water). Selective saturation of the protein resonances (on resonance spectrum) was performed by irradiating at −0.9 ppm using Gaussian-shaped

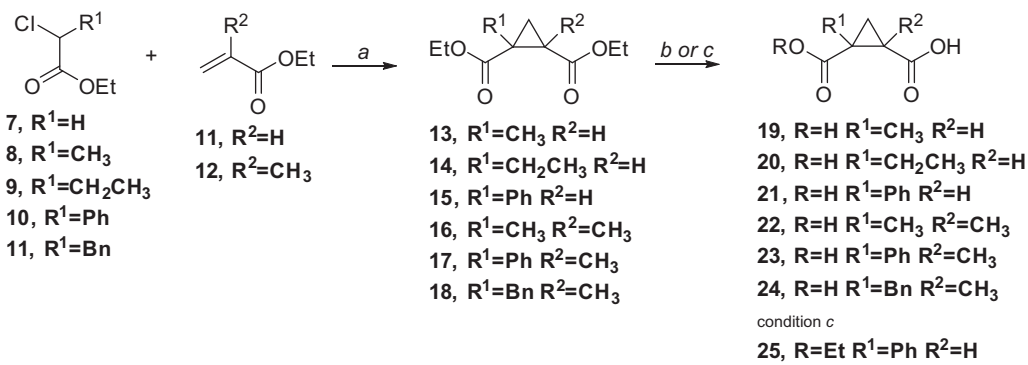

Scheme 2. [a]Reagents and conditions: (a) NaH, dry toluene, 20–40 °C, 36–72 h, 65–78%; (b) 1N KOH, THF/H_2O (1:2), 100 °C, 24 h, 62–75%; (c) 14N NaOH (1 equiv.), EtOH, reflux, 15 min, 64%. [b]For complete structures, see Table 1.

pulses for a saturation time of 3 s. For the reference spectrum (off resonance), the samples were irradiated at 26.6 ppm. NMR data were processed and analyzed using MestReNova 8.1 software (Santiago de Compostela, Spain). Group epitope mapping (GEM) was calculated setting the highest STD intensity to 100% and all other STD signals were calculated accordingly.

Direct determination of ligand-binding affinity to OASS

The binding affinity of ligands to OASS was determined by monitoring the increase in fluorescence emission of the PLP coenzyme following excitation at 412 nm[24,32]. Emission spectra were recorded as a function of ligand concentration in a solution containing 0.5–1.0 μM OASS, 100 mM Hepes buffer, pH 7.0, at 20 °C. Fluorescence measurements were carried out using a FluoroMax-3 fluorometer (HORIBA), equipped with a thermostatted cell holder, and spectra were corrected for blank contribution. The dependence of the fluorescence intensity at 500 nm on ligand concentration was fitted to a binding isotherm.

Competitive ligand-binding assays

Competitive ligand-binding assays were carried out in a similar way to the direct binding assays with the difference that the titration was carried out on an enzyme solution saturated with a low-affinity compound and the decrease in the fluorescence emission of the cofactor was followed as a function of high-affinity ligand concentration. The dependence of the fluorescence emission of the cofactor on the ligand concentration was fitted to a binding isotherm to calculate an apparent dissociation constant ($K_{d,app}$). $K_{d,app}$ is transformed into the intrinsic K_d by Equation (1) that takes into account the presence of a competing ligand for binding to the active site.

$$K_d = \frac{K_{d,\,app}}{1 + \frac{[L_{low}]}{K_d^{low}}} \quad (1)$$

$[L_{low}]$ is the low-affinity ligand concentration and K_d^{low} is the dissociation constant for the low-affinity ligand.

Docking studies

Docking studies were performed by means of the Glide9.1 suite (https://www.schrodinger.com) and using a previously refined *St*OASS-A structure[26]. The protein structure was prepared by applying the protein preparation protocol available in Maestro9.1 (https://www.schrodinger.com). The grid was cantered on the corresponding residues defining in *St*OASS-A, the Ile267-hosting pocket. The docking runs were carried out using the standard precision (SP) method; the van der Waals scaling factor of nonpolar atoms (with an absolute partial charge less than 0.15) was set to 0.8. Compound **23** was built using the fragment-built tool available in Maestro9.1 (https://www.schrodinger.com). Finally, the computationally derived G.E.M were calculated using an in-house built script.

Results and discussion

Rational design and SAR of OASS inhibitors

We have recently developed a series of substituted 2-phenylcyclopropane carboxylic acids that bound with high affinity to both the isoforms of *Salmonella enterica* serovar typhimurium OASS (*St*OASS)[27]. The main chemical feature was represented by the presence of a carboxylic acid moiety linked through a cyclopropane spacer, to a hydrophobic side chain in a *trans* configuration. These structures were rationally designed based on the *Haemophilus influenzae* (*H. influenzae*) SAT (*Hi*SAT) native C-terminal pentapeptide MNLNI, which is the natural inhibitor of OASS, and the substituent at position C-2 was represented by a small alkenyl chain, as in the case of compound **29** (Figure 1)[25]. In a second round of optimization, the alkenyl chain was embodied into a phenyl ring[30], maintaining the *trans* stereo-relationship with the carboxylic moiety. This modification led to improved synthetic feasibility and stability, and the insertion of a phenyl ring expanded the scope for further manipulation to modulate activity and drug-likeness. A vigorous improvement of compound **30** was obtained through the insertion, at the position C-1 of the cyclopropane, of hydrophobic appendages such as the ethyl, the phenylethyl and, in particular, the substituted benzyl. These modifications culminated in the synthesis of derivative **31** (Figure 1), which showed K_ds in the nanomolar range toward both *St*OASS-A and B (Figure 1). In this work, we further expand the SAR around these 2-phenylcyclopropane carboxylic acid derivatives by exploring how substitution at the C-2 or disubstitution at both C-1 and C-2 of the basic 2-phenylcyclopropanecarboxylic acid core could affect the binding affinity to *St*OASS-A and B.

First, we decided to insert a carboxylic moiety at the C-2 position taking into account that: (a) the use of polar moieties might have been beneficial in order to improve the drug-likeness of the molecules prepared. It is known that an optimal hydrophilic–lipophilic balance (HLB) may enable best penetration across Gram-negative outer membrane[33–35]; therefore, a polar moiety lowering the ClogP can be used to facilitate penetration through *S. typhimurium* cell wall; (b) serine racemase, a PLP-dependent enzyme that shows a good structural similarity with OASS, is inhibited by a series of dicarboxylic derivatives such as modified malonates[36,37]; (c) the synthetic protocol allowing to prepare such compounds is well established and high structural variability can be obtained starting from easily available materials. First, we synthesized two close analogs of **30**, which are compounds **25** and **21**, in order to assess whether the carboxylic moiety would better work as an ester or an acid. To maintain the favorable *trans* stereo-relationship between the C-2 phenyl ring and the C-1 carboxylic moiety, the carboxylic moieties were set in a *cis* configuration. We were pleased to notice that compound **21** exhibited an affinity comparable to that of the reference compound **30** toward *St*OASS-A (**21**, K_d OASS-A = 7.4 μM; **30**, K_d OASS-A = 9.2 μM), but it was 3-fold higher than parent compound **30** toward *St*OASS-B (**21**, K_d OASS-B = 55 μM; **30**, K_d OASS-B = 148 μM). Also, as expected, both the compounds had a lower predicted log *p* than the reference compounds **30** and **31**.

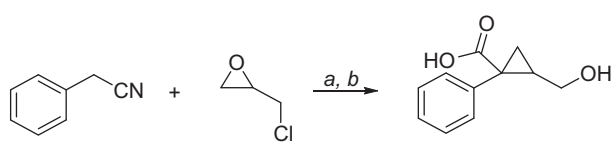

26 **27** **28**

Scheme 3. [a]Reagents and conditions: (a) $NaNH_2$, dry benzene, rt, 16 h; (b) 1N NaOH, reflux, 24 h, 35%.

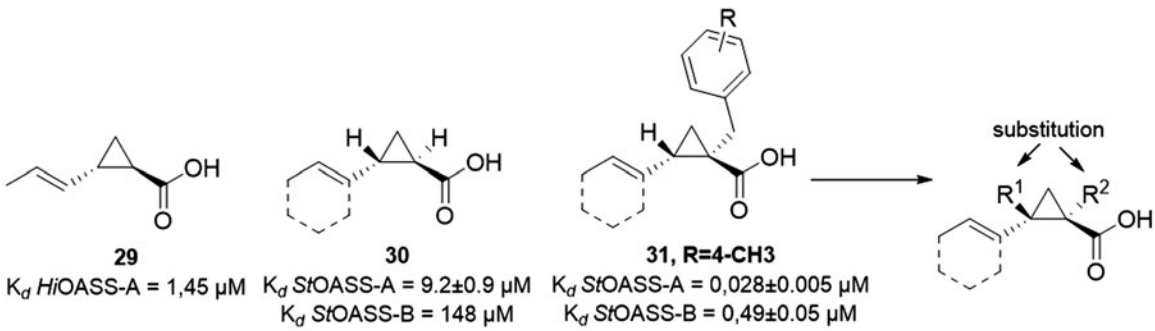

Figure 1. Evolution of cyclopropanecarboxylic acid derivatives as inhibitors of *St*OASS-A and *St*OASS-B.

At this regard, it is worthwhile to point out that inhibition of both the isoforms of the enzyme is important for granting a complete inhibition of cysteine biosynthesis in bacteria. Toward the A isoform, the ethyl ester derivative was almost 10-fold less active than the acid analog (**25**, K_d OASS-A = 83 µM), whereas the reduction in the carboxylic moiety to the corresponding alcohol (**28**, K_d OASS-A = 168 µM) led to 20-fold reduction of the affinity. This finding corroborates the importance of the acid moiety for an efficient binding to the enzyme. Puzzled by these results, we synthesized a series of derivatives to establish whether this cyclopropane-1,2-dicarboxylic acid scaffold could be considered a chemotype for *St*OASS inhibition. Based on the structure of compound **21**, a tetrasubstituted cyclopropane-1,2-dicarboxylic acid was prepared. Compound **23** showed an activity comparable to that of **21** toward the A isoform (**23**, K_d OASS-A = 9.0 µM), and, especially, it was found to be the most active derivative of this series toward the B isoform (**23**, K_d OASS-B = 40 µM). Substitution of the phenyl moiety of **23** with a benzyl appendage, led to a sharp drop in the affinity toward both the isoforms (**24**, K_d OASS-A = 48 µM; K_d OASS-B = 368 µM). Then, we wanted to reduce the size of the molecules prepared, as it is known that size, along with the HLB above mentioned, is an important characteristic in order to improve the penetration through the outer membrane of Gram-negative bacteria such as *S. typhimurium*. However, reducing the steric hindrance of the substituent at C-2, that is, substituting the phenyl ring with alkyl moieties, proved to be detrimental for the affinity. Compound **20**, bearing an ethyl moiety in place of the phenyl, showed an affinity toward *St*OASS-A in line with the derivatives described thus far (K_d OASS-A = 8.1 µM), but the affinity toward the B isoform is considerably lower than that of **21** and **23** (**20**, K_d OASS-B = 173 µM). Finally, mono- and disubstitution with a methyl group led to a considerable decrease in affinity toward the A isoform (**19**, K_d OASS-A = 49 µM; **22**, K_d OASS-A = 42 µM). Further simplification of the structure, as in the case of the unadorned cyclopropane-1,2-dicarboxylic acids, led to the least potent compounds of the series. However, despite the little affinity, synthesis of compounds **2**, **3**, **5** and **6** allowed to gain additional clues into the SAR of these derivatives. Compounds **3** and **5** showed low affinity toward the A isoform, with dissociation constants higher than 1 mM, whereas compounds **2** and **6** had a comparable binding affinity (**2**, K_d, OASS-A = 215 µM; **6**, K_d, OASS-A = 245 µM). With regard to the stereo-relationship, when the acid moieties are in a *cis* configuration, the affinity is higher with respect to the *trans* configuration. On a similar vein, when the ester moiety and the acid are in *trans* stereo-relationship, the affinity is higher than that measured on the *cis* stereoisomer. In a more comprehensive picture (Figure 2), this small set of molecules has corroborated the findings partially stemmed also from our previous studies[25,27]: assuming the cyclopropanecarboxylic acid as the pharmacophore, substituents at C-2 showing a hydrophilic character must be kept in a *cis* stereo-relationship with the C-1 carboxylic group, whereas less hydrophilic substituents must maintain a *trans* stereo-relationship.

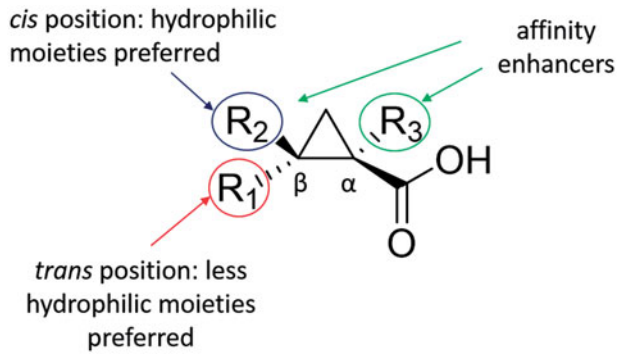

Figure 2. Preliminary SAR of cyclopropanecarboxylic acids as *St*OASS inhibitors.

Fluorescence properties of the OASS/compounds complexes

The enzymatic bioassays for this series of compounds were performed through the fluorimetric determination of the dissociation constants. This method exploits the increase in the fluorescence emission of the cofactor PLP upon ligand binding at the active site[38] and allows the direct determination of dissociation constants (i.e. the inhibition constant for competitive inhibitors). One interesting property of most compounds reported here is the high fluorescence quantum yield of the complex with either OASS-A or OASS-B (Table 1). Taking into account that the formation of the complex between the C-terminal decapeptide of SAT and OASS leads to a 4-fold increase in fluorescence emission intensity, likely due to changes in the binding pocket microenvironment and/or shielding from solvent quenching[32], some of the compounds identified in this work are far more efficient in exerting such an effect. For example, saturating concentrations of compound **19** and compound **20** lead to a 9- and 10-fold increase in the fluorescence emission of the cofactor of the A isoform (Table 1). Due to this special property, most of the compounds identified in this work could be used in competitive binding, a titration method where a low-affinity ligand is displaced from binding to a specific site by a higher affinity ligand. The physicochemical properties of complexes should be different in order to distinguish the high-affinity complex from the low-affinity one by spectroscopic or radiometric methods. This method allows the calculation of dissociation constants for tight ligands circumventing the problems associated with ligand

Table 1. Dissociation constants and fluorescence emission intensity of the title compounds for *St*OASS-A and *St*OASS-B.

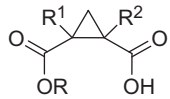

Comp	Conf*	R	R^1	R^2	K_d (μM) OASS A	K_d (μM) OASS B	SI†	F_{sat}/F_0§ OASS A	F_{sat}/F_0§ OASS B	Log P**
2	*cis*	H	H	H	215 ± 9	900 ± 90	4.2	7	3	−0.09
3	*cis*	Et	H	H	>1000	>1000	na†	na	na	0.90
5	*trans*	H	H	H	>1000	640 ± 110	<0.6	na	7	−0.09
6	*trans*	Et	H	H	245 ± 14	675 ± 9	2.8	7	5	0.90
19	*cis*	H	Me	H	49 ± 1	320 ± 20	6.5	9	4	−0.14
20	*cis*	H	Et	H	8 ± 1	173 ± 8	21	10	6	0.36
21	*cis*	H	Ph	H	7 ± 1	55 ± 3	7.4	4	5	1.08
22	*cis*	H	Me	Me	42 ± 3	350 ± 32	8.3	7	5	−0.18
23	*cis*	H	Me	Ph	9 ± 1	40 ± 2	4.4	6	7	1.04
24	*cis*	H	Me	Bn	48 ± 2	368 ± 47	7.7	5	3	1.25
25	*cis*	Et	Ph	H	83 ± 2	>1000	>12	2	4	2.07
28		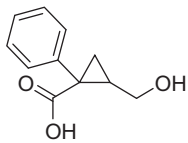			168 ± 35	nd¶	na	2	4	1.20

*Stereochemistry between the carboxylic moieties.
†SI: Selectivity index is intended as the ratio $K_{d,OASS\text{-}B}/K_{d,OASS\text{-}A}$.
‡not attainable.
¶not determined.
§the ratio between the fluorescence emission intensity at 500 nm upon excitation at 412 nm of the OASS completely saturated with the compound (F_{sat}) and the fluorescence emission intensity of the unbound OASS (F_0).
**calculated with molinspiration sotware (http://www.molinspiration.com/services/faq.html).

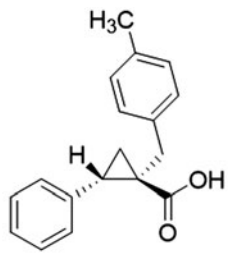

(±) 32
K_d *St*OASS-A = 0,077±0.011 μM
K_d *St*OASS-B = 1.2±0.2 μM

Figure 3. Structure of compound **32** and corresponding binding affinities.

depletion at low ligand concentrations. In fact, the presence of the low-affinity ligand allows the shifting of the apparent dissociation constant for the tight-binding ligand to higher values. Provided the low-affinity inhibitor can be added at saturating concentrations, the apparent dissociation constant for high-affinity ligand can be calculated and converted to the intrinsic dissociation constant by Equation (1) (Experimental part). This method is also convenient when the OASS/ligand complex is nonfluorescent, as is the case with compounds lacking the carboxylic moiety (BC, unpublished observation). An example of application of competitive binding assay is given in Figure 4, where the dissociation constant of the previously identified compound **32** (27) is determined by competitive binding with compound **20**.

In Figure 4(A) the spectra of the uncomplexed OASS, OASS complexed with compound **32** and OASS complexed with compound **20** are reported. The titration with compound **32** of an OASS-A solution saturated with compound **20** leads to a decrease in the fluorescence emission at 500 nm upon excitation at 412 nm (Figure 4B). The decrease in fluorescence emission is due to the displacement of compound **20** by compound **32**. The decrease in fluorescence emission can be fitted to a binding isotherm to determine the apparent dissociation constant ($K_{d,app}$) that is transformed into the intrinsic dissociation constant (K_d) using Equation (1). The calculated K_d for compound **32** is 78 ± 6 nM, in very good agreement with the published dissociation constant of 77 ± 11 nM calculated by fitting to the equation for tight binding the dependence of the fluorescence emission of OASS-A on the concentration of compound **32**.

STD-NMR analysis

In our previous investigations, we carried out a series of saturation transfer difference (STD) NMR measurements, in order to define the interaction between a given ligand and the enzyme[39]. The analysis of the STD-NMR spectra allows mapping the ligand protons directly involved in the interaction with the enzyme[40]. Once the interaction is characterized, in order to make the results readily measurable, the saturation received by the ligand protons is expressed as group epitope mapping (GEM), setting the highest saturated proton of each ligand (the closest to the enzyme) as 100%[41]. The other STD signals were calculated accordingly, yielding information on the proximity of each proton to the binding pocket of *St*OASS-A and *St*OASS-B. The STD methods suffer from some restrictions, one of which being the inability to investigate either very strong or very weak binders. In our

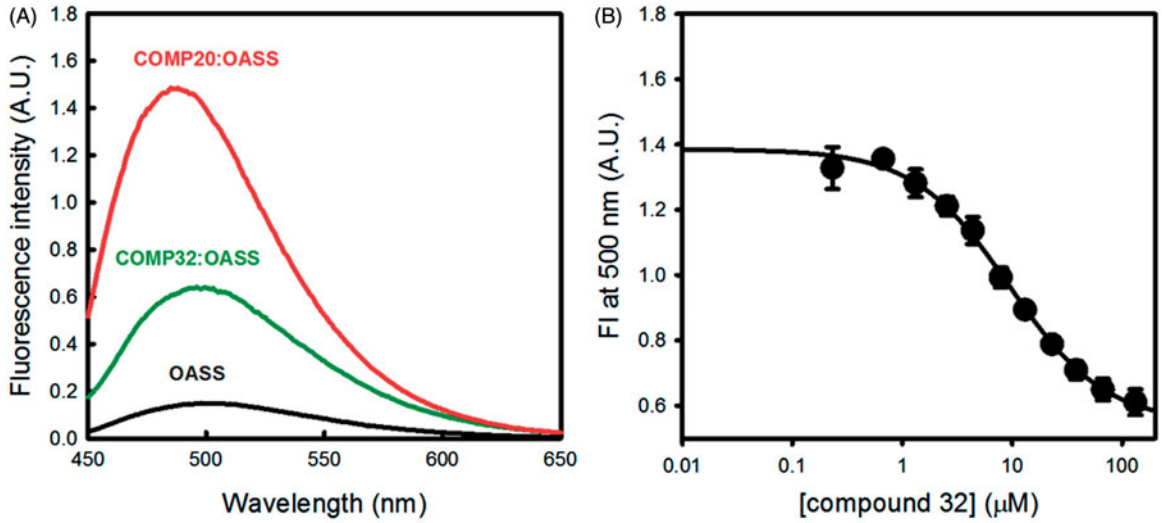

Figure 4. Use of compound **20** in a competitive binding assay for the determination of the dissociation constant of compound **32**. Panel A: fluorescence emission spectra of OASS-A upon excitation at 412 nm in the absence of ligands and in the presence of either the low affinity ligand compound **20** or the high-affinity ligand compound **32**. Panel B: displacement titration of OASS-A:compound **20** (960 μM) complex with compound **32**. The concentration of OASS used is 0.5 μM. The solid line represents the fit with a binding isotherm with an apparent dissociation constant of 9.4 ± 0.7 μM.

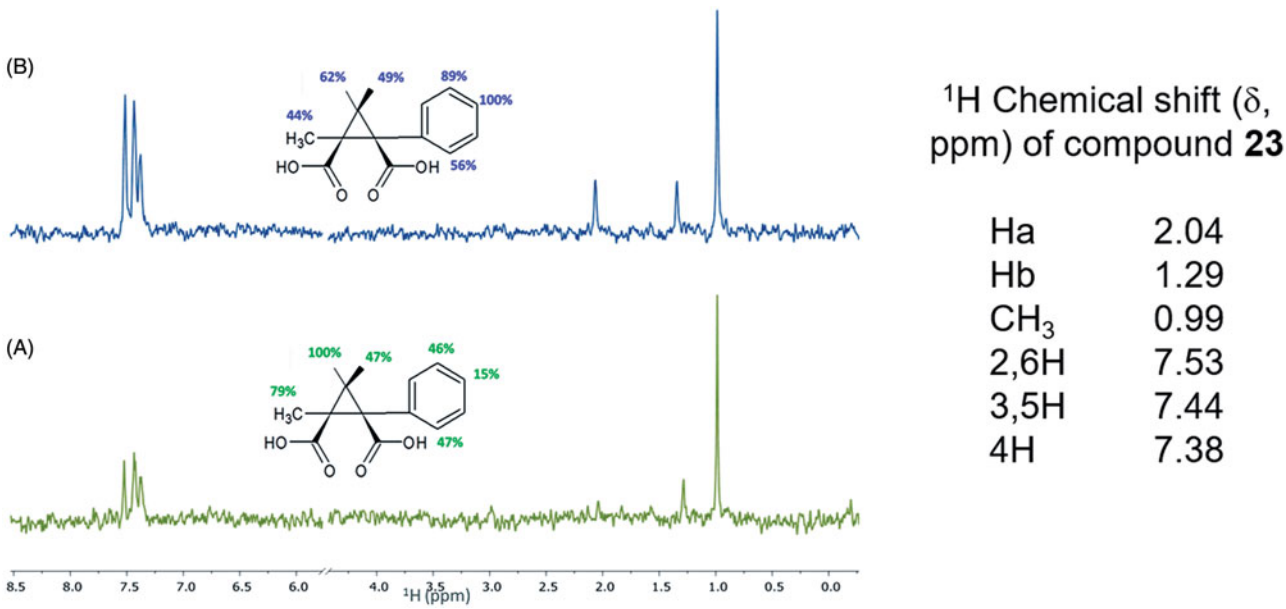

Figure 5. STD effects measurement for compound **23** in complex with *St*OASS-A (panel A) and StOASS-B (panel B). The relative degree of individual protons saturation are plotted into the structure.

previous work, this drawback led to evaluate the interaction of a ligand only with *St*OASS-A[27]. In this work, we have focused our attention on compound **23** for the following reasons: (a) the K_ds for this compound, both toward OASS-A and OASS-B, were in the suitable interval for STD-NMR experiments (K_d OASS-A = 9.0 μM; K_d OASS-B = 40 μM); (b) the structural features of **23** allowed for a rapid identification of the peaks and, also, (c) this compound was amenable for further chemical manipulation and eventually improvement.

The first information derived from this study (Figure 5) is that the same molecule exhibits different interaction modes with the two enzymes. Although this result is generally predictable due to the difference in K_ds values; in this case, it was possible to determinate which part of the molecule is mainly involved in the interaction. It can be speculated that, for *St*OASS-A, the cyclopropane spacer is positioned very close to the surface of the binding pocket. Indeed, the GEM values for protons Ha and Hb are 47% and 100%, respectively. In addition, the protons of the methyl group that is in a *cis* stereorelationship with Hb, showed a GEM value of 79%; This corroborates the importance of the cyclopropane backbone in the interaction of the molecules with the target. Therefore, in agreement with the data already reported, the cyclopropane is a good scaffold in order to properly arrange the molecule at the binding site. The design of further analogs will rely on maintaining Hb unsubstituted, given its strong proximity to the receptor surface.

Regarding *St*OASS-B, it can be seen from the GEM values of H4 (100%) and H3,5 (89%) that the protons belonging to the phenyl ring establish the strongest van der Waals interactions with the receptor surface. This evidence can somehow explain the fact

that those compounds bearing a phenyl ring at the C-2 of the cyclopropane core (i.e. **21** and **23**) bind to *St*OASS-B with dissociation constants in the tens of micromolar range, whereas compounds in which the phenyl portion is abolished (**19**, **20** and **22**), or in which it is spatially rearranged (i.e. compound **24**), show a several fold lower affinity. Altogether, the possibility to apply STD-NMR analysis to both the *St*OASS isoforms has provided a series of hints about the molecular recognition by each binding site, and this information can be exploited for the rational design of analogs able to inhibit the two enzymes in a selective or unselective fashion.

Computational analysis of 23/StOASS interaction

Since for the most active compounds the main structural motif (the 2-phenylcyclopropylcarboxylic moiety) is maintained, it can be reasonably assumed that the binding mode of these derivatives is similar to that already reported in our previous works[25–27]. To ascertain this hypothesis, and to correlate the data obtained from the STD-NMR experiments and the biochemical evaluation, a computational analysis of the binding mode of compound **23** with *St*OASS-A was performed.

The docking (Figure 6A) clearly shows that the key interactions already described are maintained also with the cyclopropane-1,2-dicarboxylic acids[25,27]. In particular, (i) the carboxylic group in position C-1 H-bonds the NH protons of Asn71 and Thr72 backbone residues; (ii) the carboxylic group in position C-2 H-bonds Asn69; and (iii) the phenyl ring in position C-2 is located in a hydrophobic pocket as previously reported, establishing a π-π parallel displaced interaction with Phe143. Therefore, the docking model that we have herein developed is in good agreement both with the SAR described in this work and with that previously reported. Finally, the selected binding mode also qualitatively recapitulates the experimentally determined GEM values (Figure 6B). Indeed, comparing the experimental GEM (green boxes, Figure 6B) with those computationally derived from the binding mode reported in Figure 6(A) (orange boxes, Figure 6B), it is clear that Ha and the CH_3 hydrogens are the atoms establishing the most relevant interactions upon inhibitor binding; the Hb, 2,6H and 3,5H hydrogens show equivalent contacts with the *St*OASS-A-active site; on the contrary, the 4H hydrogen is the least involved in the protein binding. Therefore, this further corroborates the data derived from the STD-NMR experiments.

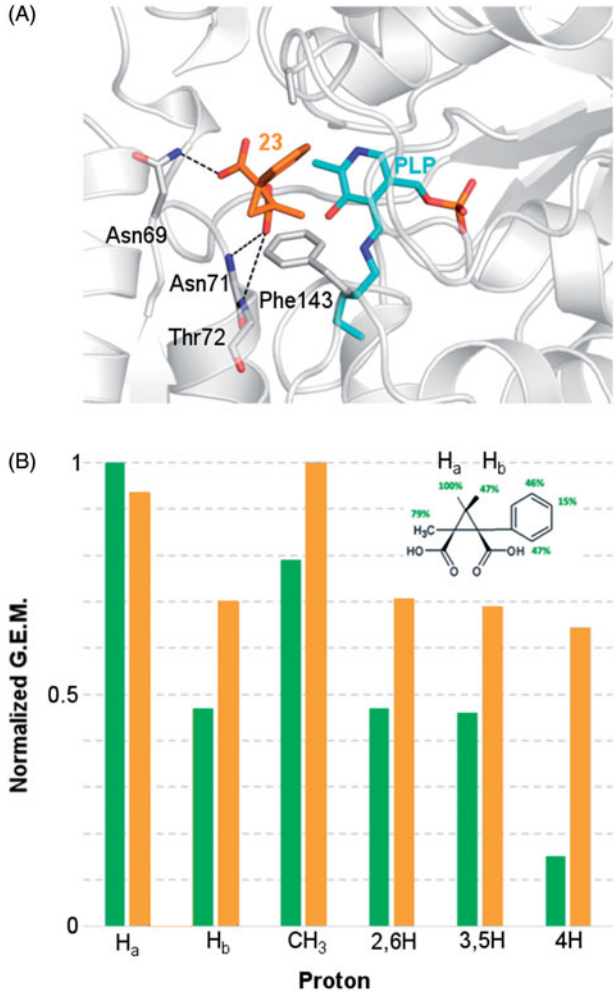

Figure 6. (A) Binding mode of compound **23** into the *St*OASS-A active site. Highlighted the Lys41-PLP adduct. (B) Experimentally (left boxes) *vs.* computationally (right boxes) derived GEM values. The values were normalized.

Experimental part

General information

All the reagents were purchased from Sigma-Aldrich, Alfa-Aesar and Enamine at reagent purity and, unless otherwise noted, were used without any further purification. Dry solvents used in the reactions were obtained by distillation of technical grade materials over appropriate dehydrating agents. MCRs were performed using CEM Microwave Synthesizer-Discover model. Reactions were monitored by thin layer chromatography on silica gel-coated aluminum foils (silica gel on Al foils, SUPELCO Analytical, Sigma-Aldrich, St. Louis, MO) at 254 and 365 nm. Where indicated, intermediates and final products were purified by silica gel flash chromatography (silica gel, 0.040–0.063 mm), using appropriate solvent mixtures.

^{1}H-NMR and ^{13}C-NMR spectra were recorded on a BRUKER AVANCE spectrometer at 300 and 100 MHz, respectively, with TMS as internal standard. ^{1}H-NMR spectra are reported in this order: multiplicity and number of protons. Standard abbreviations indicating the multiplicity were used as follows: s = singlet, d = doublet, dd = doublet of doublets, t = triplet, q = quadruplet, m = multiplet and br = broad signal. HPLC/MS experiments were performed with an Agilent 1100 series HPLC apparatus, equipped with a Waters Symmetry C18, 3.5 µm, 4.6 mm × 75 mm column and an MS: Applied Biosystem/MDS SCIEX instrument, with API 150EX ion surce. HRMS experiments were performed with an LTQ ORBITRAP XL THERMO apparatus. All compounds were tested as 95% purity or higher (by HPLC/MS). Compounds **2**[42], **3**[43], **5**[44], **6**[45] were prepared according to published protocols, and the analytical data match with those already reported.

General procedure for the synthesis of esters 13–18

To a stirred suspension of sodium hydride (60% suspension in mineral oil, 1.1 equiv) in anhydrous toluene (2 mL/mmol), the suitably substituted ethyl 2-halocarboxylate (1 equiv) and ethyl 2-acrylate (1 equiv) were added under nitrogen atmosphere at room temperature. The reaction mixture is allowed to stir at a temperature maintained between 20 and 40 °C until consumption of the starting reagents according to TLC (usually 36–72 h). The reaction is quenched by cautious addition of a small amount of methanol (1 mL) and then poured into ice-water and extracted with Et_2O (3 × 10 mL). The combined organic layers are then washed with brine, dried over $MgSO_4$, and concentrated under reduced pressure. The crude residue was purified by flash

chromatography eluting with a mixture of petroleum ether/ethyl acetate in variable proportion, to give the desired product as a white solid in yields ranging from 65% to 78%. Analytical data for compounds **13** and **16** matched the data already published[46].

Cis (±)-diethyl 1-methylcyclopropane-1,2-dicarboxylate[13]

Purified by flash column chromatography, eluent petroleum ether/ethyl acetate 90:10. Yield: 68% (pale oil); ^{1}H-NMR ($CDCl_3$ 300 MHz): δ 1.15 (s, 3H); 1.21–1.29 (*m*, 6H); 1.32–1.36 (*m*, 1H); 1.63–1.66 (*m*, 1H); 2.00–2.12 (*m*, 1H); 4.12–4.19 (*m*, 4H); LRMS (ESI) calculated for $C_{10}H_{16}O_4$ ([M-H]$^-$) 200.10; found 200.23.

Cis (±)-diethyl 1-ethylcyclopropane-1,2-dicarboxylate[14]

Purified by flash column chromatography, eluent petroleum ether/ethyl acetate 90:10. Yield: 65% (pale oil); ^{1}H-NMR ($CDCl_3$ 300 MHz): δ 1.11 (*t*, $J = 8.34$, 3H); 1.21–1.29 (*m*, 6H); 1.34–1.38 (*m*, 1H); 1.97–2.06 (*m*, 2H); 2.15–2.21 (*m*, 2H); 4.12–4.19 (*m*, 4H); LRMS (ESI) calculated for $C_{11}H_{18}O_4$ ([M-H]$^-$) 214.12; found 214.16.

Cis (±)-diethyl 1-phenylcyclopropane-1,2-dicarboxylate[15]

Purified by flash column chromatography, eluent petroleum ether/ethyl acetate 90:10. Yield: 77% (yellow oil); ^{1}H-NMR ($CDCl_3$ 300 MHz): δ 1.23–1.30 (*m*, 6H); 1.41–1.45 (*m*, 1H); 2.24–2.27 (*m*, 2H); 4.23–4.27 (*m*, 4H); 7.36−7.43 (*m*, 5H); LRMS (ESI) calculated for $C_{15}H_{18}O_4$ ([M-H]$^-$) 262.12; found 262.30.

Cis (±)-diethyl 1,2-dimethylcyclopropane-1,2-dicarboxylate[16]

Purified by flash column chromatography, eluent petroleum ether/ethyl acetate 80:20. Yield: 78% (pale oil); ^{1}H-NMR ($CDCl_3$ 300 MHz): δ 1.15 (s, 6H); 1.31–1.36 (*m*, 6H); 2.21–2.25 (*m*, 2H); 4.21–4.26 (*m*, 4H); LRMS (ESI) calculated for $C_{11}H_{18}O_4$ ([M-H]$^-$) 214.12; found 214.16.

Cis (±)-diethyl 1-methyl-2-phenylcyclopropane-1,2-dicarboxylate[17]

Purified by flash column chromatography, eluent petroleum ether/ethyl acetate 95:5. Yield: 77% (pale oil); ^{1}H-NMR ($CDCl_3$ 300 MHz): δ 1.17 (s, 3H); 1.30–1.35 (*m*, 6H), 2.17–2.21 (*m*, 2H); 4.31–4.36 (*m*, 4H); 7.32–7.38 (*m*, 5H). LRMS (ESI) calculated for $C_{16}H_{20}O_4$ ([M-H]$^-$) 276.14; found 276.33.

Cis (±)-diethyl 1-benzyl-2-methylcyclopropane-1,2-dicarboxylate[18]

Purified by flash column chromatography, eluent petroleum ether/ethyl acetate 90:10. Yield: 71% (yellowish solid); ^{1}H-NMR (CDCl3 300 MHz): δ 1.15 (s, 3H), 1.34–1.38 (*m*, 6H), 1.93–2.00 (*m*, 2H); 2.19–2.23 (*m*, 2H); 4.35–4.39 (*m*, 4H); 7.48–7.56 (*m*, 5H); LRMS (ESI) calculated for $C_{17}H_{22}O_4$ ([M-H]$^-$) 290.15; found 290.30.

General procedure for the synthesis of derivatives 19–24

To a solution of the substituted ethyl cyclopropanedicarboxylic ester (1 equiv), dissolved in a mixture of THF/water (1:2) at 0 °C, a solution of aqueous potassium hydroxide 1N (1 mL/mmol) was added dropwise. The reaction mixture was stirred at 50 °C until consumption of the starting material according to the TLC, and then acidified to pH 3 with 1N HCl. The aqueous phase was extracted with Et_2O (3 × 10 mL), and the combined organic layers were washed with brine, dried over $MgSO_4$, and concentrated under reduced pressure, to afford the title compound as a white solid in yields ranging from 62% to 75%. The products underwent biological assays without any further purification. Following a similar procedure, but using equimolar amount of KOH and EtOH as the solvent, title compound **25** was obtained from **15** in 64% yield. Analytical data for compounds **19** and **22** matched those already published[46].

Cis (±)-1-methylcyclopropane-1,2-dicarboxylic acid[19]

Purified by filtration and washed with Et_2O. Yield: 70% (white powder); ^{1}H-NMR ($CDCl_3$ 300 MHz): δ 1.13 (s, 3H); 1.23–1.26 (*m*, 1H); 1.51–1.56 (*m*, 1H); 2.13–2.17 (*m*, 2H). ^{13}C-NMR (100.6 MHz, $CDCl_3$): 33.21; 31.41; 23.54; 16.54. HRMS (ESI) calculated for $C_6H_8O_4$ ([M-H]$^-$) 144.0425; found 144.1388.

Cis (±)-1-ethylcyclopropane-1,2-dicarboxylic acid [20]

Purified by filtration and washed with Et_2O. Yield: 73% (white powder); ^{1}H-NMR ($CDCl_3$ 300 MHz): δ 1.11 (*t*, $J = 8.34$, 3H); 1.26–1.31 (*m*, 1H), 1.97–2.06 (*m*, 2H), 2.15–2.21 (*m*, 2H). ^{13}C-NMR (100.6 MHz, $CDCl_3$): 33.32; 31.17; 21.48; 18.49; 11.59. HRMS (ESI) calculated for $C_7H_{10}O_4$ ([M-H]$^-$) 158.0679; found 158.1500.

Cis (±)-1-phenylcyclopropane-1,2-dicarboxylic acid[21]

Purified by filtration and washed with Et_2O. Yield: 75% (white powder); ^{1}H-NMR ($CDCl_3$ 300 MHz): δ 1.40–1.44 (*m*, 1H); 2.24–2.27 (*m*, 2H), 7.33−7.39 (*m*, 5H). ^{13}C-NMR (100.6 MHz, $CDCl_3$): 129.29; 128.21; 126.87; 33.32; 31.17; 21.48. HRMS (ESI) calculated for $C_{15}H_{18}O_4$ ([M-H]$^-$) 206.0625; found 206.1912.

Cis (±)-1,2-dimethylcyclopropane-1,2-dicarboxylic acid[22]

Purified by filtration and washed with Et_2O. Yield: 75% (white powder); ^{1}H-NMR ($CDCl_3$ 300 MHz): δ 1.12 (s, 6H); 2.21–2.25 (*m*, 2H). ^{13}C NMR (100.6 MHz, $CDCl_3$): 33.32; 31.17; 21.48; 17.58. HRMS (ESI) calculated for $C_7H_{10}O_4$ ([M-H]$^-$) 158.0606; found 158.1245.

Cis (±)-1-methyl-2-phenylcyclopropane-1,2-dicarboxylic acid[23]

Purified by filtration and washed with Et_2O. Yield: 69% (white powder); ^{1}H-NMR ($CDCl_3$ 300 MHz): δ 1.21 (s, 3H); 2.12–2.15 (*m*, 2H); 7.31–7.37 (*m*, 5H). ^{13}C NMR (100.6 MHz, $CDCl_3$): 129.18; 128.33; 126.67; 31.17; 17.58. HRMS (ESI) calculated for $C_{12}H_{12}O_4$ ([M-H]$^-$) 220.0712; found 220.2035.

Cis (±)-1-benzyl-2-methylcyclopropane-1,2-dicarboxylic acid[24]

Purified by filtration and washed with Et_2O. Yield: 62% (white powder); ^{1}H-NMR ($CDCl_3$ 300 MHz): δ 1.21 (s, 3H); 1.94–2.03 (*m*, 2H); 2.21–2.25 (*m*, 2H); 7.41–7.49 (*m*, 5H). ^{13}C-NMR (100.6 MHz, $CDCl_3$): 131.123; 129.56; 126.32; 33.54; 17.34; 11.23. HRMS (ESI) calculated for $C_{13}H_{14}O_4$ ([M-H]$^-$) 234.0985; found 234.1158.

Cis (±)-2-(ethoxycarbonyl)-2-phenylcyclopropanecarboxylic acid[25]

Purified by flash column chromatography eluting petroleum ether/ethyl acetate 90:10. Yield: 64% (white powder); ^{1}H-NMR ($CDCl_3$ 300 MHz): δ 1.21–1.25 (*t*, $J = 7.54$, 3H); 1.65–1.67 (*m*, 1H); 2.33–2.35 (*m*, 2H); 4.11–4.16 (*m*, 2H); 7.33–7.37 (*m*, 5H). ^{13}C NMR (100.6 MHz, $CDCl_3$): 130.12; 129.67; 127.44; 33.54;

32.23; 17.54; 11.13. HRMS (ESI) calculated for $C_{13}H_{14}O_4$ ([M-H]$^-$) 234.0920; found 234.2102.

Synthesis of 2-(hydroxymethyl)-1-phenylcyclopropane-1-carboxylic acid[28]

A solution of benzyl cyanide (2.0 g, 17.1 mmol) was added dropwise over 30 min to a suspension of $NaNH_2$ (1.54 g, 39.3 mmol) in benzene at 0 °C. After stirring for 3 h at room temperature, a solution of epichloroydrin (1.53 g, 16.6 mmol) was added to the reaction mixture over 45 min, using an ice-bath to keep the temperature in a range between 20 and 40 °C. After consumption of the limiting reagent, monitored by TLC, 1N NaOH (16.6 mL) is cautiously added dropwise to the reaction mixture that is allowed to react at 90 °C overnight. After cooling, the benzene was decanted, and the acqueous phases was extracted with dichloromethane (3 × 20 mL), acidified with 2N HCl to pH 2 and extracted again with ethyl acetate (3 × 10 mL). The combined organic layers were then washed with brine, dried over $MgSO_4$ and concentrated under reduced pressure. The crude residue was purified by flash chromatography eluting with petroleum ether/ethyl acetate (90:10), to give the desired product as a white solid in 35% overall yield. ^{1}H-NMR ($CDCl_3$ 300 MHz): δ 1.74–1.78 (*m*, 1H); 1.88–1.94 (*m*, 2H); 3.98–4.03 (*m*, 2H); 7.44–7.58 (*m*, 5H). ^{13}C-NMR (100.6 MHz, $CDCl_3$): 130.24; 129.86; 128.21; 33.61; 32.84; 15.16. HRMS (ESI) calculated for $C_{11}H_{12}O_3$ ([M-H]$^-$) 192.0898; found 192.2011.

Conclusions

Inhibition of cysteine biosynthesis may affect the life cycle of many unicellular microorganisms and plants. The enzyme *O*-acetylserine sulfhydrylase catalyzes the last step of cysteine biosynthesis, and, as such, it can be considered an interesting target for future drug development. Combining computational and spectroscopic approaches such as fluorescence and saturation transfer difference (STD) NMR, we have previously reported a series of 2-phenylcyclopropane carboxylic acids highly active on *St*OASS-A and *St*OASS-B. In this paper, we have further refined the SAR around this scaffold in order to build compounds that are more likely to penetrate through the outer membrane of Gram-negative bacteria. In this work, a novel pattern of substitutions, so far unexplored for this nucleus, was investigated. In particular, taking the previously reported compound **30** as the template, disubstitution at the position C-2 and C-1 through the addition of small functional groups was carried out. The synthesis of substituted cyclopropane-1,2-dicarboxylic acids proved to be a valuable structural solution; therefore, a small series of analogs in which the two carboxylic moieties, separated by a cyclopropane linker, were maintained in the *cis* stereo-configuration was synthesized and tested. One special feature of many compounds within this series is the high fluorescence quantum yield of their complexes with OASS. This property makes these compound suitable tools for the determination of the affinity of OASS ligands by competitive ligand-binding assays. Analyzing the results of binding experiments, the small set of molecules has highlighted the importance of the cyclopropanecarboxylic acid as the pharmacophore, and the chemical nature of the substituents at C-2, coupled to their stereo-configuration with regard to the carboxylic moiety at C-1, as determinant for strong binding. Moreover, STD NMR experiments were directed to provide hints on the binding mode of the tightest compound to *St*OASS-A and *St*OASS-B. Altogether, these findings add further information around this valuable scaffold, and represent a solid base for the synthesis of improved, drug-like and more efficient OASS inhibitors.

Acknowledgements

The Centro Interdipartimentale Misure ''G. Casnati'' is kindly acknowledged for the contribution in the analytical determination of the molecules synthesized.

Declaration of interest

The authors report no conflicts of interest. The authors alone are responsible for the content and writing of this article.

The work described in this paper was partly carried out under the MSCA-ITN-2014-ETN project INTEGRATE (grant number 642620).

References

1. Wray JL, Campbell EI, Roberts MA, Gutierrez-Marcos JF. Redefining reductive sulfate assimilation in higher plants: a role for APS reductase, a new member of the thioredoxin superfamily? Chem Biol Interact 1998;109:153–67.
2. Sekowska A, Kung HF, Danchin A. Sulfur metabolism in *Escherichia coli* and related bacteria: facts and fiction. J Mol Microbiol Biotechnol 2000;2:145–77.
3. Tai CH, Nalabolu SR, Jacobson TM, et al Kinetic mechanisms of the A and B isozymes of O-acetylserine sulfhydrylase from *Salmonella typhimurium* LT-2 using the natural and alternate reactants. Biochemistry (Mosc) 1993;32:6433–42.
4. Mozzarelli A, Bettati S, Campanini B, et al. The multifaceted pyridoxal 5′-phosphate-dependent O-acetylserine sulfhydrylase. Biochim Biophys Acta BBA – Proteins Proteomics 2011;1814:1497–510.
5. Kröger C, Colgan A, Srikumar S, et al. An infection-relevant transcriptomic compendium for *Salmonella enterica* Serovar Typhimurium. Cell Host Microbe 2013;14:683–95.
6. Kredich NM. Regulation of L-cysteine biosynthesis in *Salmonella typhimurium*. I. Effects of growth of varying sulfur sources and O-acetyl-L-serine on gene expression. J Biol Chem 1971;246:3474–84.
7. Hulanicka MD, Hallquist SG, Kredich NM, Mojica-A T. Regulation of O-acetylserine sulfhydrylase B by L-cysteine in *Salmonella typhimurium*. J Bacteriol 1979;140:141–6.
8. Croft SL, Sundar S, Fairlamb AH. Drug resistance in leishmaniasis. Clin Microbiol Rev 2006;19:111–26.
9. Senaratne RH, De Silva AD, Williams SJ, et al. 5′-Adenosinephosphosulphate reductase (CysH) protects *Mycobacterium tuberculosis* against free radicals during chronic infection phase in mice. Mol Microbiol 2006;59:1744–53.
10. Diner EJ, Beck CM, Webb JS, et al. Identification of a target cell permissive factor required for contact-dependent growth inhibition (CDI). Genes Dev 2012;26:515–25.
11. Tanous C, Soutourina O, Raynal B, et al The CymR regulator in complex with the enzyme CysK controls cysteine metabolism in *Bacillus subtilis*. J Biol Chem 2008;283:35551–60.
12. Campanini B, Benoni R, Bettati S, et al Moonlighting O-acetylserine sulfhydrylase: new functions for an old protein. Biochim Biophys Acta BBA – Proteins Proteomics 2015;1854:1184–93.
13. Ma DK, Vozdek R, Bhatla N, Horvitz HR. CYSL-1 interacts with the O2-sensing hydroxylase EGL-9 to promote H2S-modulated hypoxia-induced behavioral plasticity in *C. elegans*. Neuron 2012;73:925–40.
14. Pearson MM, Yep A, Smith SN, Mobley HLT. Transcriptome of proteus mirabilis in the murine urinary tract: virulence and nitrogen assimilation gene expression. Infect Immun 2011;79:2619–31.
15. Turnbull AL, Surette MG. L-Cysteine is required for induced antibiotic resistance in actively swarming *Salmonella enterica* serovar typhimurium. Microbiol Read Engl 2008;154:3410–19.
16. Turnbull AL, Surette MG. Cysteine biosynthesis, oxidative stress and antibiotic resistance in *Salmonella typhimurium*. Res Microbiol 2010;161:643–50.
17. Wang Q, Frye JG, McClelland M, Harshey RM. Gene expression patterns during swarming in *Salmonella typhimurium*: genes specific to surface growth and putative new motility and pathogenicity genes. Mol Microbiol 2004;52:169–87.
18. Stec J, Huang Q, Pieroni M, et al Synthesis, biological evaluation, and structure–activity relationships of *N*-benzoyl-2-hydroxybenzamides as agents active against *P. falciparum* (K1 strain), trypanosomes, and leishmania. J Med Chem 2012;55:3088–100.

19. Singh P, Brooks JF, Ray VA, et al CysK plays a role in biofilm formation and colonization by *Vibrio fischeri*. Appl Environ Microbiol 2015;81:5223–34.
20. Campanini B, Pieroni M, Raboni S, et al Inhibitors of the sulfur assimilation pathway in bacterial pathogens as enhancers of antibiotic therapy. Curr Med Chem 2015;22:187–213.
21. Jean Kumar VU, Poyraz Ö, Saxena S, et al Discovery of novel inhibitors targeting the *Mycobacterium tuberculosis* O-acetylserine sulfhydrylase (CysK1) using virtual high-throughput screening. Bioorg Med Chem Lett 2013;23:1182–6.
22. Salsi E, Campanini B, Bettati S, et al A two-step process controls the formation of the bienzyme cysteine synthase complex. J Biol Chem 2010;285:12813–22.
23. Salsi E, Bayden AS, Spyrakis F, et al Design of O-acetylserine sulfhydrylase inhibitors by mimicking nature. J Med Chem 2010;53: 345–56.
24. Spyrakis F, Singh R, Cozzini P, et al Isozyme-specific ligands for O-acetylserine sulfhydrylase, a novel antibiotic target. PLoS One 2013; 8:e77558.
25. Amori L, Katkevica S, Bruno A, et al Design and synthesis of trans-2-substituted-cyclopropane-1-carboxylic acids as the first non-natural small molecule inhibitors of O-acetylserine sulfhydrylase. Med Chem Comm 2012;3:1111.
26. Bruno A, Amori L, Costantino G. Computational insights into the mechanism of inhibition of OASS-A by a small molecule inhibitor. Mol Inform 2013;32:447–57.
27. Pieroni M, Annunziato G, Beato C, et al Rational design, synthesis, and preliminary structure-activity relationships of α-substituted-2-phenylcyclopropane carboxylic acids as inhibitors of *Salmonella typhimurium* O-acetylserine sulfhydrylase. J Med Chem 2016;59:2567–78.
28. Zhao Q, Wong HNC. Synthetic studies toward plakortide E: application of the Feldman oxygenation to synthesis of highly substituted 1,2-dioxolanes. Tetrahedron 2007;63:6296–305.
29. McCoy LL. Three-membered rings. The preparation of some 1,2-cyclopropanedicarboxylic acids. J Am Chem Soc 1958;80:6568–72.
30. Pieroni M, Annunziato G, Azzali E, et al Further insights into the SAR of α-substituted cyclopropylamine derivatives as inhibitors of histone demethylase KDM1A. Eur J Med Chem 2015;92:377–86.
31. Beato C, Pecchini C, Cocconcelli C, et al Cyclopropane derivatives as potential human serine racemase inhibitors: unveiling novel insights into a difficult target. J Enzyme Inhib Med Chem 2016;31: 645–52.
32. Campanini B, Speroni F, Salsi E, et al Interaction of serine acetyltransferase with *O*-acetylserine sulfhydrylase active site: evidence from fluorescence spectroscopy. Protein Sci 2005;14:2115–24.
33. Denyer SP, Maillard J-Y. Cellular impermeability and uptake of biocides and antibiotics in Gram-negative bacteria. J Appl Microbiol 2002;92:35S–45S.
34. Brown DG, May-Dracka TL, Gagnon MM, Tommasi R. Trends and exceptions of physical properties on antibacterial activity for Gram-positive and Gram-negative pathogens. J Med Chem 2014;57: 10144–61.
35. Zgurskaya HI, López CA, Gnanakaran S. Permeability barrier of Gram-negative cell envelopes and approaches to bypass it. ACS Infect Dis 2015;1:512–22.
36. Strísovský K, Jirásková J, Mikulová A, et al Dual substrate and reaction specificity in mouse serine racemase: identification of high-affinity dicarboxylate substrate and inhibitors and analysis of the beta-eliminase activity. Biochemistry (Mosc) 2005;44: 13091–100.
37. Goto M, Yamauchi T, Kamiya N, et al Crystal structure of a homolog of mammalian serine racemase from *Schizosaccharomyces pombe*. J Biol Chem 2009;284:25944–52.
38. McClure GD, Cook PF. Product binding to the alpha-carboxyl subsite results in a conformational change at the active site of O-acetylserine sulfhydrylase-A: evidence from fluorescence spectroscopy. Biochemistry (Mosc) 1994;33:1674–83.
39. Benoni R, Pertinhez TA, Spyrakis F, et al Structural insight into the interaction of O-acetylserine sulfhydrylase with competitive, peptidic inhibitors by saturation transfer difference-NMR. FEBS Lett 2016;590:943–53.
40. Mayer M, Meyer B. Characterization of ligand binding by saturation transfer difference NMR spectroscopy. Angew Chem Int Ed 1999; 38:1784–8.
41. Mayer M, Meyer B. Group epitope mapping by saturation transfer difference NMR to identify segments of a ligand in direct contact with a protein receptor. J Am Chem Soc 2001;123:6108–17.
42. Neumeyer JL, Zhang A, Xiong W, et al. Design and synthesis of novel dimeric morphinan ligands for kappa and micro opioid receptors. J Med Chem 2003;46:5162–70.
43. de la Fuente Revenga M, Balle T, Jensen AA, Frølund B. Conformationally restrained carbamoylcholine homologues. Synthesis, pharmacology at neuronal nicotinic acetylcholine receptors and biostructural considerations. Eur J Med Chem 2015;102: 352–62.
44. Wang F, Xu XY, Wang FY, et al An efficient and improved process for the scale-up preparation of cis-cyclopropanediamine dihydrochloride. Lett Org Chem 2015;12:741–4.
45. Hugentobler KG, Rebolledo F. Enantioselective bacterial hydrolysis of amido esters and diamides derived from (±)-trans-cyclopropane-1,2-dicarboxylic acid. Org Biomol Chem 2014;12: 615–23.
46. Kaur K, Aeron S, Bruhaspathy M, et al Design, synthesis and activity of novel derivatives of oxybutynin and tolterodine. Bioorg Med Chem Lett 2005;15:2093–6.